International Journal of Computational Vision and Biomechanics
Vol. 5 No. 1 (January-June, 2019)

MUK PUBLICATIONS
Open Access Publisher

Material Properties and Extended Sources for Surface Rendering

Jan J. Koenderink & Sylvia C. Pont

Department of Physics and Astronomy, Universiteit Utrecht, The Netherlands

Submitted: 27th October 2018 *Revised: 25th December 2018* *Accepted: 17th January 2019*

We consider generic BRDFs (Bidirectional Reflectance Distribution Functions) for rendering material surface properties. This is of importance in diverse graphics applications. Of various formal proposals found in the literature many are not plausible *because they violate one or more physical constraints on BRDFs and of the plausible ones it is often unknown whether they are* feasible, i.e., *whether an exact physical model exists. Apart from the (default) Lambertian case, no analytical examples from the literature are* conservative *(*i.e.*. remit all of the incident light). We investigate the simplest types of plausible BRDF that mimick the generic lobes commonly encountered in the daily environment: diffuse lobe (sand, paper, …), specular lobe (smooth plastic, brushed metal, …), backscatter lobe (rough plaster, lawn, …) and asperity scattering lobe (velvet, hairy or dusty surfaces, …). We propose novel methods to handle not just collimated, but also diffuse and ambient light beams for arbitrary surface rendering. These methods allow rendering of plausible "material properties" with no more overhead than the familiar "Lambertian surface illuminated by point source at infinity with ambient term". The results are exact for convex objects, though only approximate in more complicated cases.*

Keywords: BRDF, material rendering, diffuse beams, extended sources, scientific visualization.

INTRODUCTION

In scientific visualization one often uses "shading" to augment the visual impression of three–dimensionality of mere outline graphics [11]. In order to do so one has to simulate light sources and the way photons are bounced off the surfaces.

With "local rendering" we imply the determination of the radiance of the beam scattered towards the eye in the absence of such multilocal effects as cast shadowing and multiple scattering (reflexes). The most general case where local rendering is exact is that of arbitrarily illuminated convex objects. In this paper we restrict the radiation to beams due to sources at (effective) infinity, though this is not an essential constraint. The simplest implementation of the irradiating beam involves a "point source at infinity" and the simplest implementation of scattering the "Lambertian surface" [19,5]. More "realistic" implementations consider "extended sources" [29] and general BRDFs.

As is well known from photography, in order to suggest both shape and material properties one needs strategically placed extended sources and characteristic, non–Lambertian BRDFs [22]. This is awkward from the perspective of computer graphics implementation since standard graphics pipelines assume point sources and Lambertian surfaces. For "cheap rendering" the choice of suitable BRDFs and extended sources are critical in computer graphics.

EXTENDED SOURCES

An "extended source" is fully described through the radiance of the incident beam [4]. Let $\mathbf{n}$ denote the unit surface normal, $\mathbf{i}$ the direction towards an infinitesimal element of the source, $N_i(\mathbf{i})$ the radiance. Then the irradiance $H(\mathbf{n})$ of a surface element is

$$H(\mathbf{n}) = \int_{\mathbf{i}\cdot\mathbf{n}>0} (\mathbf{i}\cdot\mathbf{n})\, N_i(\mathbf{i})\, d\mathbf{i},$$

where $d\mathbf{i}$ denotes an infinitesimal vector solid angle in the direction of $\mathbf{i}$. The irradiance depends upon the spatial attitude of the surface element with respect to the incident beam through the "Lambert cosine Law" ($\mathbf{i}$. $\mathbf{n}$).

For the purposes of this paper we consider only three extreme types of incident beams, namely the *collimated beam* (often—rather awkwardly—called "point source at infinity"), the *hemispherical diffuse beam* with a total angular spread of 2π steradians, and the *Ganzfeld* with a total angular spread of 4π steradians. The collimated beam is a good model for direct sunlight (actual angular spread 6×10^{-5} steradians), the hemispherical diffuse beam for overcast sky (though we take the sky radiance as uniform instead of decreasing by about a factor of three from zenith to horizon), and the Ganzfeld for "ambient light" (a pure Ganzfeld exists only in circumstances like the "polar white–out").

Collimated beam Consider a surface element with unit (outward) normal $\mathbf{n}$, irradiated from the direction (unit vector) $\mathbf{i}$ and viewed from the direction (unit vector) $\mathbf{j}$. Let the normal irradiance caused by the incident beam be H_0, then the irradiance is $H(\mathbf{i}, \mathbf{n}) = H_0\, \mathbf{i} \cdot \mathbf{n}$ (by Lambert's law). The radiance arriving at the eye is proportional with the irradiance, thus $N(\mathbf{i}, \mathbf{j}, \mathbf{n}) = f(\mathbf{i}, \mathbf{j}, \mathbf{n})\, \mathrm{H}(\mathbf{i}, \mathbf{n})$. Here the function $f(\mathbf{i}, \mathbf{j}, \mathbf{n})$ is the "bidirectional reflectance distribution function (BRDF)". Notice that $\mathbf{i} \cdot \mathbf{n} \in [0, 1]$, whereas $\mathbf{i} \cdot \mathbf{n} \leq 0$ implies "body shadow". (For an overview of recommended terminology see [1].)

Hemispherical diffuse beam Consider a surface that is irradiated with a hemispherical diffuse beam of radiance $N(\mathbf{k}) = N_i$ for $\mathbf{i} \cdot \mathbf{k} > 0$ and zero otherwise. The "direction" of

the beam is **i**. The radiance ofthe scattered beam is (notice that you may take $\mathbf{i}\cdot\mathbf{n}\in[-1,+1]$ here!):

$$N_j(\mathbf{i},\mathbf{j},\mathbf{n}) = \int_{(\mathbf{i}\cdot\mathbf{n}>0)\wedge(\mathbf{i}\cdot\mathbf{k}>0)} (\mathbf{k}\cdot\mathbf{n}) N_i(\mathbf{k})\, f(\mathbf{k},\mathbf{j},\mathbf{n})\, d\mathbf{k} = N_i\, g(\mathbf{i},\mathbf{j},\mathbf{n}).$$

The function g (**i**, **j**, **n**) sums up the effect of self–occultation (or "vignetting") of the source, so it may be called the "Law of Vignetting". For a white, Lambertian surface you obtain $g_L(\mathbf{i},\mathbf{j},\mathbf{n}) = (1+\mathbf{i}\cdot\mathbf{n})/2$, thus the scattered radiance does not depend on the viewing direction **j**. In the Lambertian case the result is reminescent to the "point source at infinity with ambient light" formula. This is a mere accidental fact that applies only to the Lambertian case and does not generalize to general surfaces (*vide infra*).

Fully diffuse beam: "Ganzfeld" Since the incident radiance is independent of direction, the integrand depends only on the nature of the BRDF. One has

$$N_j(\mathbf{j},\mathbf{n}) = N_i \int_{\mathbf{i}\cdot\mathbf{n}>0} (\mathbf{i}\cdot\mathbf{n})\, f(\mathbf{i},\mathbf{j},\mathbf{n})\, d\mathbf{i} = N_i\, h(\mathbf{j},\mathbf{n}).$$

Thus the scattered radiance depends only on the viewing direction **j**. In analogy with the case of radiation seeping out of a translucent medium one might call $h(\mathbf{j},\mathbf{n})$ the "Law of Darkening" [7]. For a white Lambertian surface the law of darkening is $h_L = 1$. Thus a white Lambertian surface becomes *invisible* in a Ganzfeld whereas a convex, gray Lambertian surface is rendered as a uniform silhouette. For general BRDFs the law of darkening is not constant and characteristic of the material though. Thus in general the contribution due to "ambient light" is not an additive constant as it is in the case of Lambertian surfaces. In order to render correctly one has to precompute the proper law of darkening for any material in the scene.

In general the case of diffuse beams is very complicated, since one has to perform a double integration for each location. The use of a canonical beam, such as the hemispherical diffuse beam, allows one to use a function of three directions instead. This is convenient, since **i**, **j** and **n** are available in the graphics pipeline. Thus it really saves much computation to stick to canonical illuminations and analytical BRDFs.

Notice that the material (scattering) properties of a surface are conveniently summed up in terms of three functions, namely

— the "Law of Shading" $f(\mathbf{i},\mathbf{j},\mathbf{n})$,
— the "Law of Vignetting" $g(\mathbf{i},\mathbf{j},\mathbf{n})$, and
— the "Law of Darkening" $h(\mathbf{j},\mathbf{n})$.

A convenient measure of the "lightness" of a surface is the double diffuse reflectance, that is the fraction of a fully diffuse beam (Ganzfeld) scattered into any direction. One has

$$r = \frac{1}{\pi}\int_{\mathbf{j}\cdot\mathbf{n}>0}\int_{\mathbf{i}\cdot\mathbf{n}>0} (\mathbf{i}\cdot\mathbf{n})(\mathbf{j}\cdot\mathbf{n})\, f(\mathbf{i},\mathbf{j},\mathbf{n})\, d\mathbf{i}\, d\mathbf{j}.$$

For the Lambertian surface $r_L = 1$, this surface is a perfect scatterer. For a surface that is not a perfect scatterer ("not conservative") is it useful to define the "albedo" as the function $a(\mathbf{i},\mathbf{n}) = \int_{\mathbf{j}\cdot\mathbf{n}>0} (\mathbf{j}\cdot\mathbf{n})\, f(\mathbf{i},\mathbf{j},\mathbf{n})\, d\mathbf{j}$. Because of "Helmholtz reciprocity" (see below) one has that $a(\mathbf{k},\mathbf{n}) = h(\mathbf{k},\mathbf{n})$. Apparently $r = \frac{1}{\pi}\int_{\mathbf{i}\cdot\mathbf{n}>0} (\mathbf{i}\cdot\mathbf{n}) a(\mathbf{i},\mathbf{n})\, d\mathbf{i}$. For the Lambertian white surface $a_L = 1$, in general $a(\mathbf{i},\mathbf{n}) \le 1$, due to the requirement of conservation of radiant flux.

For purposes of rendering in collimated and diffuse light fields surfaces are fully described through the functions $f(\mathbf{i},\mathbf{j},\mathbf{n})$, $g(\mathbf{i},\mathbf{j},\mathbf{n})$, $h(\mathbf{j},\mathbf{n})$, whereas $a(\mathbf{i},\mathbf{n})$ and r characterize overall reflecting properties. For the Lambertian surface you have the simple expressions ($f_L = 1/\pi$, $g_L(\mathbf{i},\mathbf{n}) = (1+\mathbf{i}\cdot\mathbf{n})/2$ and $h_L, a_L, r_L = 1$) that are usually implemented in rendering pipelines (see figure 1). For more general surfaces these functions can be almost arbitrarily complicated. This is no problem in practice though since they may be precomputed and frozen in lookup tables.

BRDFS

"Default" material properties are Lambertian [19], but often one prefers a "more realistic" type of surface material with a certain degree of gloss, *etc*. This introduces the problem of theoretical (analytic or algorithmic) surface scattering, typically handled via special BRDFs [1,25]. Often such BRDFs are chosen for computational convenience [11], rather than physical plausibility. Many shading algorithms in common use implement physically impossible surface scattering properties [2, 3, 27]. Attempts to replace these with physically realistic alternatives meet with perhaps unexpected problems. For instance, it is very hard to conceive of "interesting" (that is different from the default Lambertian) analytical expressions that would simulate *physically admissible* surface scattering properties and that are also *conservative*, *i.e.*, that scatter all incident photons without absorbing any.

Notice that the Lambertian BRDF (the generic instance) is *plausible* in the sense that it does not violate known physical constraints (non–negativity, Helmholtz reciprocity and energy conservation, *vide infra*), but that it is unknown whether it is also *feasible*. A BRDF may be called "feasible" if there exists a model surface that yields that BRDF in terms of geometrical optics. (For examples [18,8, 33].) Although we can easily check BRDFs on plausibility, we can less easily check them on feasibility. Attempts to "explain" the Lambertian BRDF have been going on since the 18th century [5], but so far all have failed. The BRDFs known to be feasible have all started out as models (e.g., the perfect mirror, *etc*.) of particular physical surfaces [16,28], not as *ad hoc* postulated analytical expressions.

General Properties of BRDFs

The BRDF is a property of a surface. It is clearly non–negative throughout. General arguments suggest that the

BRDF is a symmetrical function in the directions of the entrance and exit beams, so called "Helmholtz reciprocity" [25, 21, 14, 18]. For a surface area A the incident radiant power is $H(\mathbf{i}, \mathbf{n})A$, whereas the total remitted radiant power is

$$\int_{(2\pi)} N(\mathbf{i},\mathbf{j},\mathbf{n})\, d\varepsilon = \int_{(2\pi)} N(\mathbf{i},\mathbf{j},\mathbf{n})(\mathbf{j}\cdot\mathbf{n})A\, d\mathbf{j}.$$

Here $d\varepsilon$ is the element of étendue (or throughput), and $d\mathbf{j}$ is an element of solid angle in the direction of $\mathbf{j}$. The symbol (2π) denotes integration over the hemisphere $\mathbf{j}\cdot\mathbf{n} \geq 0$. Since the surface is assumed to (perhaps) absorb radiation, but emit none, conservation of energy requires that the "albedo" $a(\mathbf{i},\mathbf{n}) \leq 1$. A "conservative" surface is a surface of "unit albedo", that is one that remits all radiation falling upon it, irrespective the direction of the entrance beam. These exhaust all constraints on the BRDF that are listed in the literature:

$$f(\mathbf{i},\mathbf{j},\mathbf{n}) \geq 0 \qquad \textit{non-negativity} \tag{1}$$

$$f(\mathbf{i},\mathbf{j},\mathbf{n}) = f(\mathbf{j},\mathbf{i},\mathbf{n}) \quad \textit{Helmholtz reciprocity} \tag{2}$$

$$a(\mathbf{i},\mathbf{n}) \leq 1 \qquad \textit{"conservation of energy"} \tag{3}$$

Although there are several BRDFs in use that "conserve energy [20]" none of them has unit albedo except for the Lambertian case. In this paper we restrict the term "energy conservation" solely to the case of unit albedo. The final inequality is then simply a necessary condition for a BRDF to be counted as "plausible".

A great many BRDFs in common use fail to be plausible [20]. Although this is known to violate basic radiometry such BRDFs are used because of algorithmic speed or ease of implementation in hardware graphics pipelines. Many users prefer speed over realism that they "can't see". Perhaps the most popular choices are the Phong [27] and the Blinn–Phong [2,3] BRDFs. Neither of these are plausible though because they violate Helmholtz reciprocity.

Generic, Simple, Analytic BRDFs

One can easily frame plausible BRDFs through simple analytic expressions. Many are simple enough that they pose no problems of algorithmic speed or ease of implementation. We suggest useful examples below.

The major modes of surface scattering are *bulk scattering*, *specular reflection*, *backscattering* and *asperity scattering*. Together (and in various combinations) these account for most of the materials encountered in the daily human environment. Exceptions involve macroscopic or microscopic deterministic structure [34,35,36] (coombed hair, opals, peacock feathers), we ignore these. The generic scattering modes give rise to more or less well defined "lobes" in the scattering indicatrix, often easily identified in empirically determined BRDFs.

Bulk scattering is due to photons that did enter the bulk of the material and emerge after multiple (sub–surface) scattering events [26, 7]. After such multiple scattering events all traces of the direction of incidence are wiped out. This results in a broad, diffuse lobe centered on $\mathbf{n}$. Almost any material shows some bulk scattering;

Specular reflection is due to Fresnel reflection at planar interfaces between materials of different refractive index [4,14]. Often the surface is only locally planar, but macroscopically or mesoscopically "bumpy". In such cases one observes a lobe that is roughly centered on $\mathbf{k} = 2(\mathbf{i}\cdot\mathbf{n})\mathbf{n} - \mathbf{i}$, that is the direction of the mirror–reflected ray, but broadened due to the bumpiness [32,12]. The degree of broadening can vary enormously. In some cases (lemon–peel for instance) the lobe has stochastic structure due to sparse sampling of the bumpiness;

Backscattering is typical for rough surfaces [18]. The combined influence of cast shadowing and visual occlusion (both due to vignetting) makes that only illuminated parts of the surface are seen from the direction of incidence [31,22] ("heiligenschein"). One obtains a rather broad lobe centered on $\mathbf{i}$. This is why the full moon is so bright [13,22] (for that reason called "opposition effect");

Asperity scattering is due [17,10] to a layer of asperities that cover the nominal surface like a thin "atmosphere". Common examples are human skin or plant leaves covered with tiny hairs, the tips of which act as asperities. Dust or face powder has a similar effect. Synthetic examples include various types of velvet. Peaches are optically different from plums due to asperity scattering. One has a typically narrow lobe extended along the surface, orthogonal to $\mathbf{n}$.

Models of various complexity (and physical realism) can be framed for any of these modes. Usually one has insufficient knowledge concerning a surface to actually apply a full blown physical model though. There is a room for simple analytical expressions that manage to capture the essence of the major modes. One may regard them as "phenomenological models" since they not necessarily respect all kinds of physical constraints. We will only consider plausible models though.

Since we require the BRDFs to be plausible, they have to be non–negative functions of the basic constituents:

$$f_\star(\mathbf{i},\mathbf{j},\mathbf{n}) = 1,$$

$$f_\star(\mathbf{i},\mathbf{j},\mathbf{n}) = \frac{1}{2}(1+\mathbf{i}\cdot\mathbf{j}),$$

$$f_\star(\mathbf{i},\mathbf{j},\mathbf{n}) = \frac{1}{2}(\mathbf{i}+\mathbf{j})\cdot\mathbf{n},$$

$$f_\star(\mathbf{i},\mathbf{j},\mathbf{n}) = ((\mathbf{i}\cdot\mathbf{n})(\mathbf{j}\cdot\mathbf{n})).$$

Notice that these parts are all in the range [0, 1], thus they are not to be considered BRDF's as such. Since the parts satisfy Helmholtz reciprocity, any function of them will too. The scalar product $\mathbf{i}\,.\,\mathbf{j}$ captures the similarity between the directions of exit and incidence and thus allows one to capture the geometry of backscattering. Likewise, the product $((\mathbf{i}\cdot\mathbf{n})(\mathbf{j}\cdot\mathbf{n}))$ allows one to capture the geometry

of asperity scattering. In order to capture the characteristic properties of the "lobes" we only consider unimodal BRDFs. All cases are illustrated in figure 1.

For typical materials the BRDF is multimodal and determined by a combination of bulk scattering ("diffuse reflectance"), specular reflectance ("gloss"), backscattering and asperity scattering [9]. Such combinations can be constructed by "partitive mixture of BRDFs", that is to say

$$f(\mathbf{i},\mathbf{j},\mathbf{n}) = \frac{\sum_{k=1}^{N} \mu_k f_k(\mathbf{i},\mathbf{j},\mathbf{n})}{\sum_{k=1}^{N} \mu_k}.$$

One easily shows that such a mixture is non–negative throughout, conforms to Helmholtz reciprocity and does not violate energy conservation if this applies to the individual components. The method is well suited to be combined with a method suggested by Ngan *et al.* [24] for image driven BRDF selection.

Bulk Scattering

The best known (and most frequently used) instance of bulk scattering is of course the Lambertian surface. There doesn't exist a physical model, so the Lambertian BRDF is a phenomenological model. It does not fit cases of actual diffuse scattering particularly well, especially in the cases of grazing directions of incidence or viewing [23,26]. In order to correct for this Minnaert [22] suggested the expression ("*d*" for "diffuse")

$$f_d(\mathbf{i},\mathbf{j},\mathbf{n}) = C_d\left((\mathbf{i}\cdot\mathbf{n})(\mathbf{j}\cdot\mathbf{n})\right)^{\xi}, \text{ with } C_d = \frac{2+\xi}{2\pi}.$$

The parameter ξ controls the degree of "edge darkening". The parameter ξ may take any positive values, but realistic values are in the range from zero to one. For $\xi = 0$ the Minnaert BRDF turns into the Lambertian, a realistic value for use is $\xi = 1$. The value of the constant C_d has been chosen to be the maximum value that does not violate energy conservation. This simple but instructive case allows us to introduce some important notions. The Minnaert BRDF produces a lobe centered upon the surface normal, irrespective of the direction of the incident beam. The radiance in directions that graze the surface is zero. Thus an object rendered with a Minnaert BRDF will have a dark edge, different from the Lambertian case.

The Law of Vignetting can be found analytically by straightforward integration, but is complicated, because expressed in terms of confluent hypergeometric functions [6]:

$$g_d(\mathbf{i},\mathbf{j},\mathbf{n}) = \frac{\Gamma(\frac{3+\xi}{2})}{\sqrt{\pi}\Gamma(1+\frac{\xi}{2})}(\mathbf{i}\cdot\mathbf{n})(\mathbf{j}\cdot\mathbf{n})^{\xi}\ {}_2F_1(\frac{1}{2},-\frac{\xi}{2},\frac{3}{2},(\mathbf{i}\cdot\mathbf{n})^2),$$

for integer α

$$g_d(\mathbf{i},\mathbf{j},\mathbf{n}) = \frac{\Gamma(\frac{3+\xi}{2})}{\xi\sqrt{\pi}\Gamma(\frac{\xi}{2})}(\mathbf{j}\cdot\mathbf{n})^{\xi}\ B_{(\mathbf{i}\cdot\mathbf{n})^2}(\frac{1}{2},1+\frac{\xi}{2}),$$

where B_z denotes the incomplete beta–function. Simple expressions are obtained for small integer exponents, *e.g.*, for $\xi = 1$ one has:

$$g_d(\mathbf{i},\mathbf{j},\mathbf{n}) = \frac{\mathbf{j}\cdot\mathbf{n}}{\pi}\left(\pi - \arccos(\mathbf{i}\cdot\mathbf{n}) + \mathbf{i}\cdot\mathbf{n}\sqrt{1-(\mathbf{i}\cdot\mathbf{n})^2}\right).$$

Thus it is indeed different from the Lambertian expression. In the case of the Lambertian BRDF the rendering function is equal to that for a "point source at infinity with ambient light", but we now see that this is fortuitous. The law of darkening can also be obtained in closed form, namely $h_d(\mathbf{j},\mathbf{n}) = (\mathbf{j}\cdot\mathbf{n})^{\xi}$. It depends on the value of the edge darkening parameter. (See figure 2) Apparently the Minnaert BRDF is not conservative, indeed the albedo for collimated illumination is $a_d = (\mathbf{i}\cdot\mathbf{n})^{\xi}$. Since $a_d < 1$ for $\xi > 0$ the Minnaert surface does not scatter all photons, but absorbs some. The surface is as bright as the constraints allow, yet scatters less effectively than the Lambertian surface. The double diffuse reflectance is $r_d = 2/(2+\xi)$.

Specular reflection

A simple expression for a specular lobe is ("s" stands for "specular"):

$$f_s(k,\mathbf{i},\mathbf{j},\mathbf{n}) = C_s\left(\frac{1+\mathbf{k}\cdot\mathbf{j}}{2}\right)^{\alpha}$$
$$= C_s\left(\frac{1}{2}+(\mathbf{i}\cdot\mathbf{n})(\mathbf{j}\cdot\mathbf{n})-\frac{\mathbf{i}\cdot\mathbf{j}}{2}\right)^{\alpha} \text{ with } C_s(k) = \frac{(1+\alpha)(2+\alpha)}{2\pi(2\alpha+2^{-\alpha})},$$

where we limit α to positive integer values. The expression captures the mirror reflection in the simplest possible way. An expression due to Lewis [20] (known as "cosine lobe" illumination model) is very similar, but fails to be non–negative and when this is cured turns out to have as purious lobe (due to the original negative part). The above expression is unimodal by design. Again, the normalization factor C_s has been chosen to be as large as is compatible with energy conservation. This BRDF has a single lobe in the direction of the reflected ray. The width of the lobe can be controlled through the parameter α. Realistic values run from $\alpha = 1$ (a dull gloss) to very high (looks more specular). The illustration is for $\alpha = 8$. Although the Law of Vignetting and the Law of Darkening can be obtained in terms of elementary functions for integer values of $\alpha > 0$, the resulting expressions contain so many terms that they are practically useless for realistic values of the parameter. It is a simple matter to precalculate a lookup table of course. The BRDF is not conservative, *e.g.*, the albedo is $a_s = (3+2\mathbf{i}\cdot\mathbf{n})/5$ for $\alpha = 1$, and $a_s =$

$$\frac{(24201945+33554432\cos\theta+9773400\cos 2\theta-415212\cos 4\theta+10728\cos 6\theta-45\cos 8\theta)}{67125248},$$

for $\alpha = 8$, where $\theta = \arccos(\mathbf{i}\cdot\mathbf{n})$. A sphere in a Ganzfeld shows a dark edge. (See figure 3).

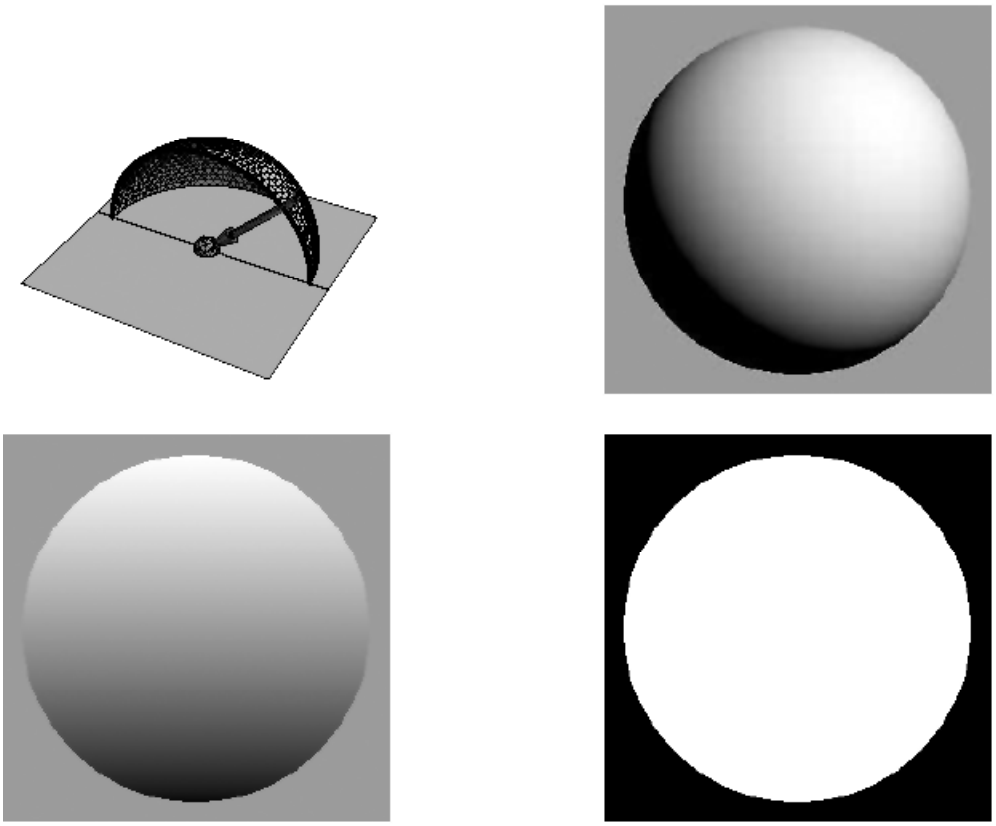

Figure 1: The Lambertian case. At top left a graphical rendering of the scattering indicatrix and right a rendering of a sphere illuminated with a collimated beam (at 45° from the viewing direction, from upper right—as indicated by the arrow). At bottom left a sphere illuminated with a hemispherical diffuse beam and right a sphere in a Ganzfeld.

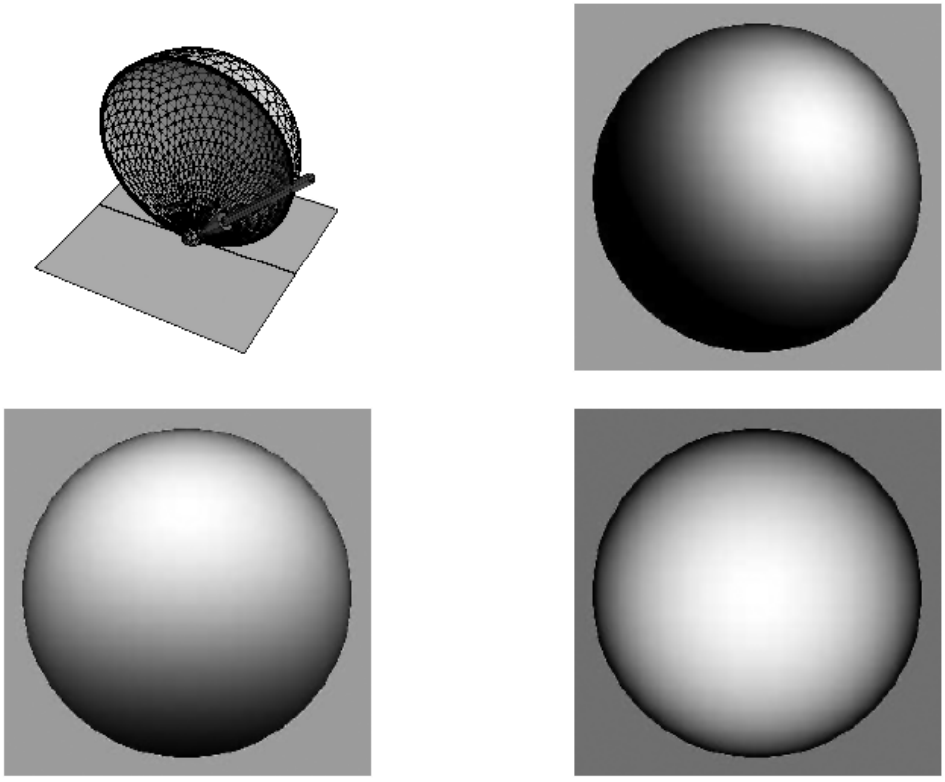

Figure 2: The Minnaert diffuse lobe for ξ = 1. At top left a graphical rendering of the scattering indicatrix and right a rendering of a sphere illuminated with a collimated beam (at 45° from the viewing direction, from upper right—as indicated by the arrow). At bottom left a sphere illuminated with a hemispherical diffuse beam and right a sphere in a Ganzfeld.

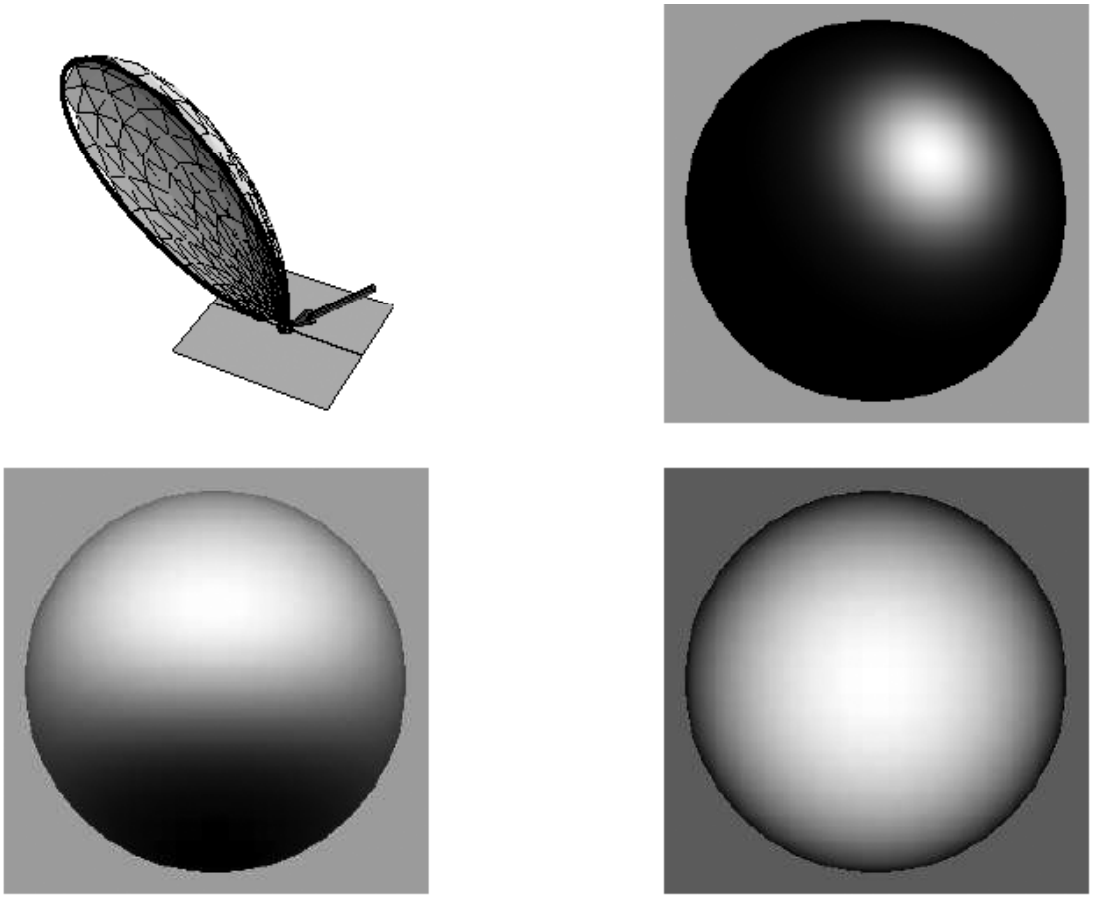

Figure 3: The specular lobe for α = 8. At top left a graphical rendering of the scattering indicatrix and right a rendering of a sphere illuminated with a collimated beam (at 45° from the viewing direction, from upper right—as indicated by the arrow). At bottom left a sphere illuminated with a hemispherical diffuse beam and right a sphere in a Ganzfeld.

Backscattering

Arguably the simplest expression that yields a true backscatter lobe is ("*b*" stands for "backscatter"):

$$f_b(k,\mathbf{i},\mathbf{j},\mathbf{n}) = C_b\left(\frac{1+\mathbf{i}\cdot\mathbf{j}}{2}\right)^{\alpha} \text{ with } C_b = \frac{6}{5\pi 2^{\alpha}},$$

where the normalizing factor C_b has been chosen to maximize the reflectance. One easily checks that the scattered beam is unimodal, its width can be controlled through the parameter α. The Law of Vignetting and the Law of Darkening can be obtained analytically for integer values of $\alpha > 0$. The resulting expressions are numerically useful for small values of α (a realistic case). For instance, for $\alpha = 1$ you have that

$$g_b(\mathbf{i},\mathbf{j},\mathbf{n}) = \frac{3}{10}(1+\cos\theta) + \frac{1}{5\pi}\left(\cos\eta - \cos(\eta+2\theta) + 2(\pi-\theta)\sin\eta\sin\zeta\right),$$

where $\mathbf{i}\cdot\mathbf{n} = \cos\theta$, $\mathbf{j}\cdot\mathbf{n} = \sin\eta\sin\zeta$ and $[\mathbf{i},\mathbf{j},\mathbf{n}] = -\cos\zeta\sin\theta$. For instance, for $\alpha = 1$ the Law of Darkening is $h_b(\mathbf{i},\mathbf{n}) = (3+2\mathbf{i}\cdot\mathbf{n})/5$. Thus the BRDF is not conservative, there is a slight edge darkening. (See figure 4).

Perhaps remarkably, it is possible to design a "perfect backscatterer", that is a surface whose reflectance in the backscatter direction does not depend upon the direction of incidence. A sphere of such a material, when viewed from the direction of the incident beam (*e.g.*, the full moon), appears like a featureless, uniform disk. A simple BRDF that achieves this is

$$f_{pb}(k,\mathbf{i},\mathbf{j},\mathbf{n}) = C_{pb}\frac{(1+\mathbf{i}\cdot\mathbf{j})^{\alpha}}{(\mathbf{i}+\mathbf{j})\cdot\mathbf{n}} \text{ with } C_{pb}(k) = \frac{1+\alpha}{2^{1+\alpha}\pi}$$

for integer $\alpha \geq 2$. We do not know whether this is the only possible BRDF with this property.

Asperity Scattering

A simple expression that yields a "surface lobe" typical of asperity scattering is ("*a*" stands for "asperity scattering"):

$$f_a(k,\mathbf{i},\mathbf{j},\mathbf{n}) = C_a\left(1-(\mathbf{i}\cdot\mathbf{n})(\mathbf{j}\cdot\mathbf{n})\right)^{\alpha} \text{ with } C_a = \frac{1}{\pi}.$$

The normalizing factor C_a is as large as possible as is compatible with the plausibility constraints. The parameter α should be larger than one. For high values of the parameter one has strong, velvet–like, asperity scattering. Notice that the expression is much like the "complementary" of the Minnaert BRDF. For any direction of incidence the radiance is highest (namely C_a) in directions grazing the surface. The

radiance falls off rapidly for less oblique rays. The parameter α controls the "'width" of the asperity scattering lobe. The Law of Vignetting and the Law of Darkening can be obtained analytically for integer values of $\alpha > 0$. For small values of α one obtains useful expressions though. For instance, for the realistic value $\alpha = 1$ one has

$$g_a(\mathbf{i},\mathbf{j},\mathbf{n}) = \frac{1+\mathbf{i}\cdot\mathbf{n}}{2} - \frac{4\mathbf{j}\cdot\mathbf{n}}{3\pi}\left(\pi - \arccos(\mathbf{i}\cdot\mathbf{n}) + \mathbf{i}\cdot\mathbf{n}\sqrt{1-(\mathbf{i}\cdot\mathbf{n})^2}\right) - \frac{1}{8}(\mathbf{j}\cdot\mathbf{n})^2(\mathbf{i}\cdot\mathbf{n}-2)(\mathbf{i}\cdot\mathbf{n}+1)^2,$$

$$h_a(\mathbf{j},\mathbf{n}) = 1 - \frac{2}{3}(\mathbf{j}\cdot\mathbf{n}).$$

The BRDF is not conservative. This material shows an edge lightening, as is typical for a material like velvet which shows strong asperity scattering. (See figure 5)

CONCLUSIONS

The literature on *ad hoc* expressions for the bidirectional reflectance distribution function is rather muddled. Even today (mainly in the computer graphics community) BRDF expressions that fail on mere plausability are in common use. Non–plausibleBRDF expressions have become scarce in applied optics after Minnaert's work. As we have shown simple analytical expressions can be framed such that no physical constraints are violated and yet such that well known generic physical properties of common materials such as diffuse scattering, specular scattering (gloss), backscattering and asperity scattering are represented in a parameterized manner. One property that cannot so easily be accommodated is conservation of radiant power though.

The choice of a few canonical surfaces and a few canonical light fields as advocated here has the merit that it is easily integrated in existing graphics pipelines with almost negligible (as compared to the Lambertian assumption) overhead, yet without violating basic physical constraints. This allows more realistic rendering to be done "on the cheap". The method is exact for convex objects, though only approximate for non–convex ones, precisely as with the standard default rendering method.

In general one will assign different colors to the various components, *e.g.*, the diffuse component is due to the bulk material and will be assigned the "body color", the backscatter component is due to multiple scattering microcavities, thus willbe assigned the body color at higher saturation level, whereas the specular and asperity components are due to directly scattered or Fresnel reflected radiation, thus will be assigned the color of the source [15, 30, 37].

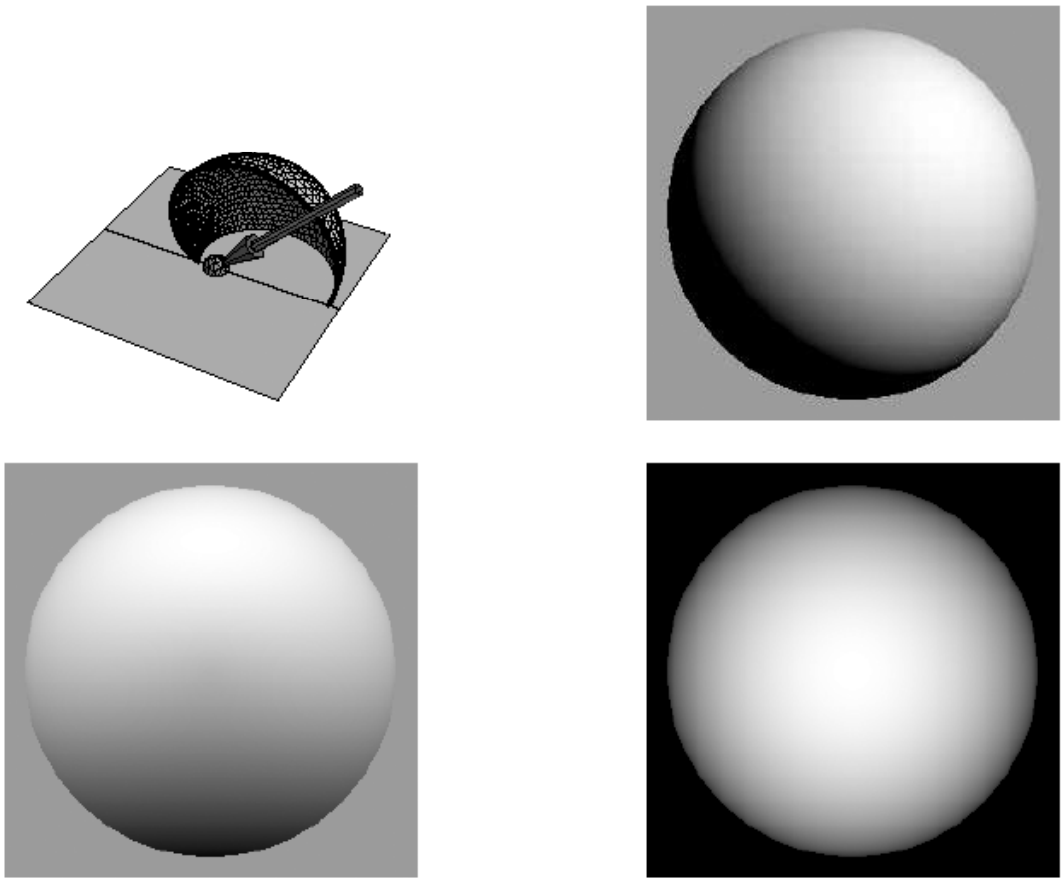

Figure 4: The backscatter lobe for $\alpha = 1$. At top left a graphical rendering of the scattering indicatrix and right a rendering of a sphere illuminated with a collimated beam (at 45° from the viewing direction, from upper right—as indicated by the arrow). At bottom left a sphere illuminated with a hemispherical diffuse beam and right a sphere in a Ganzfeld.

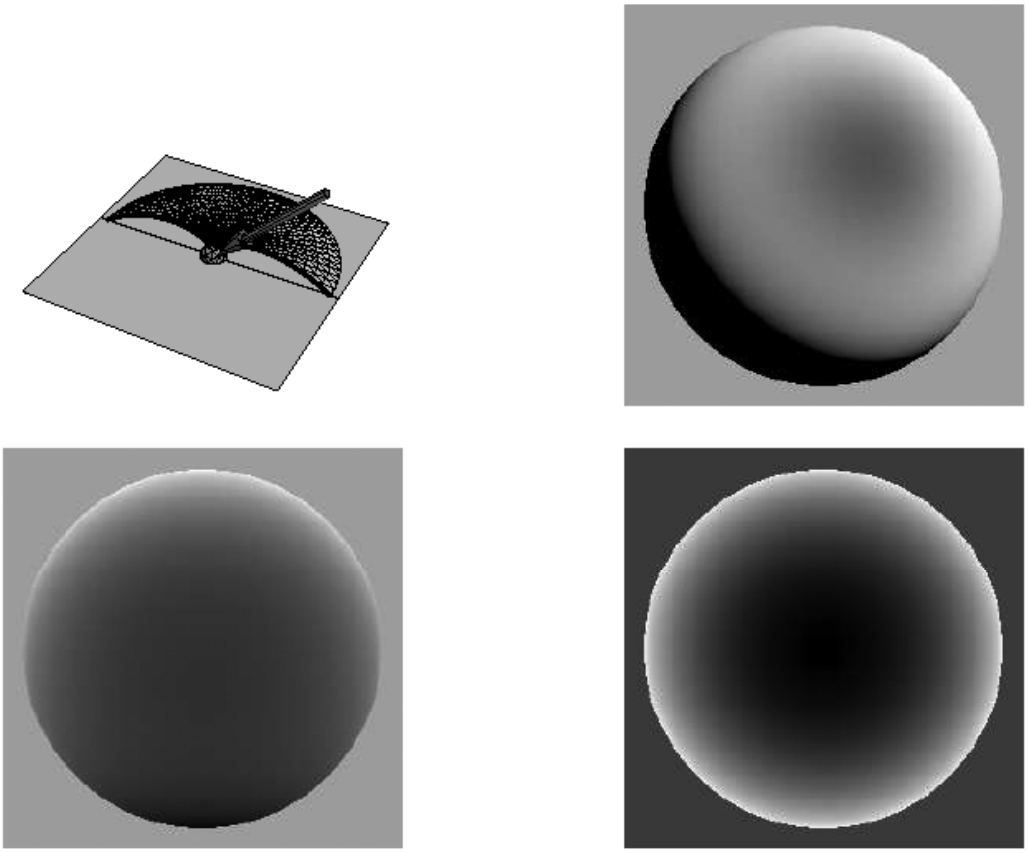

Figure 5: The asperity scattering lobe for $\alpha = 1$. At top left a graphical rendering of the scattering indicatrix and right a rendering of a sphere illuminated with a collimated beam (at 45° from the viewing direction, from upper right—as indicated by the arrow). At bottom left a sphere illuminated with a hemispherical diffuse beam and right a sphere in a Ganzfeld.

ACKNOWLEDGEMENTS

This work was sponsored via the European program Visiontrain contract number MRTNCT2004005439. Sylvia Pont was supported by the Netherlands Organisation for Scientific Research (NWO).

REFERENCES

[1] American National Standards Institute/Illuminating Engineering Society of North America, Nomenclature and definitions for illuminating engineering, ansi/ies rp–16–1986 edition, 1986.

[2] Blinn, J. F. and Newell, M. E., Texture and reflection in computer generated images, Communications of the ACM **19**, pp. 542–546, 1976.

[3] Blinn, J. F. and Newell, M. E., Models of light reflection for computer synthesized pictures, Computer Graphics (SIGGRAPH '77 Proceedings) **11**, pp. 192–198, 1977.

[4] Born, M. and Wolf, E., Principles of Optics, Cambridge University Press, Cambridge, 1998.

[5] Bouguer, P., Traité d'optique sur la gradation de la lumière, posthumous edition arranged by Nicolas Louis de la Caille, H. L. Guerin & L. F. Delatour, Paris, 1760.

[6] Buchholz, H. The Confluent Hypergeometric Function with Special Emphasis on its Applications. Springer–Verlag, New York, 1969.

[7] Chandrasekhar, S., Radiative Transfer, Dover Publications, Inc., New York, 1960.

[8] Cook, R. L. and Torrance, K. E., A reflection model for computer graphics, ACM Transactions on Graphics **1**, pp. 7–24, 1982.

[9] Dana, K. J., Van–Ginneken, B., Nayar, S. K. and Koenderink, J. J., Reflectance and Texture of Real World Surfaces, ACM Transactions on Graphics (TOG), **18**, pp. 1–34, 1999.

[10] Egan, W. G. and Hilgerman, T., Spectral reflectance of particulate materials: a Monte Carlo model including asperity scattering. Applied Optics **17**, pp. 245–252, 1978.

[11] Foley, J. D., Dam A. van, Feiner, S. K, and Hughes, J. F., Computer graphics, Principles and Practice, 2nd Ed., Addison–Wesley, Reading Massachusetts, 1990.

[12] Ginneken, B. van, Stavridi, M. and Koenderink, J. J., Diffuse and specular reflection from rough surfaces, Applied Optics **37(1)**, pp. 130–139 1998.

[13] Hapke, B., Nelson, R. and Smythe, W., The opposition effect of the moon: coherent backscatter and shadow hiding. Icarus **133**, pp. 89–97, 1998.

[14] Hecht, E., Optics, Addison–Wesley Publishing Company, Reading, Massachusetts, 2002.

[15] Klinker, G. J., Shafer, S. A. and Kanade, T., Using a color reflection model to separate highlights from object color, in: Proceedings of the First International Conference on Computer Vision, Computer Society Press of the IEEE, Washington, pp. 145–150, 1987.

[16] Koenderink, J. J., A. J. van Doorn, K. J. Dana, and S. Nayar, Bidirectional Reflection Distribution Function of thoroughly pitted surfaces, *International Journal of Computer Vision*, **31** (2/3), pp. 129-144, 1999.

[17] Koenderink, J. J. and Pont, S. C., The secret of velvety skin, Machine Vision and Applications; Special Issue on Human Modeling, Analysis and Synthesis, **14**, pp. 260–268, 2003.

[18] Kortüm, G., Reflexionsspektroskopie. Grundlagen, Methodik, Anwendungen. Springer, Heidelberg, 1969.

[19] Lambert, J. H., Photometria, sive de Mensura et gradibus luminis, colorum et umbræ, Eberhard Klett, Augsberg, 1760.

[20] Lewis, R. R., Making shaders more physically plausible, In: Fourth Eurographics Workshop on Rendering, pp. 47–62, 1993.

[21] Minnaert, M., The reciprocity principle in lunar photometry, *Astrophysical Journal* **93**, pp. 403–410, 1941.

[22] Minnaert, M., The Nature of Light and Colour in the Open Air Dover, New York, 1954.

[23] Nayar, S. K. and Oren, M., Visual appearance of matte surfaces, Science **267**, pp. 1153–1156, 1995.

[24] Ngan, A., Durand, F. and Matusik, W., Image–driven navigation of analytical BRDF models, Eurographics Symposium on Rendering 2006, Eds., Akenine–Möller and Wolfgang Heidrich, 2006.

[25] Nicodemus, F. E., Richmond, J. C., Hsia, J. J., Ginsberg, I. W. and Limperis, T., Geometric considerations and nomenclature for reflectance, Natl. Bur. Stand. (U. S.) Monogr. **160** (U. S.. Department of Commerce, Washington D. C.), 1977.

[26] Oren, M. and Nayar, S. K., Generalization of the Lambertian model and implications for machine vision, *International Journal of Computer Vision* **14**, pp. 227–251, 1995.

[27] Phong, B. T., Illumination for computer generated pictures, Communications of the ACM **18**, pp. 311–317, 1975.

[28] Pont, S. C., and Koenderink, J. J. BRDF of specular surfaces with hemispherical pits, *Journal of the Optical Society of America* A **19**, pp. 2456–2466, 2002.

[29] Pomraning, G. C., The Equations of Radiation Hydrodynamics, Pergamon Press, Oxford, 1973.

[30] Shafer, S. A., Using color to separate reflection components," Color Research Applications **10**, pp. 210–218, 1985.

[31] Schlichting, H. J. and Uhlenbrock, M., Der Heiligenschein als NaturerScheinung, Physik in unserer Zeit, **3**, pp. 173–175, 1999.

[32] Torrance, K. E. and Sparrow, E. M., Theory of off–specular reflection from roughened surfaces, *Journal of the Optical Society of America* **57**, pp. 1105–1114, 1967.

[33] Torrance, K. E., Sparrow, E. M. and Birkebak, R. C., Polarization, directional distribution, and off-specular peak phenomena in light reflected from roughened surfaces, *Journal of the Optical Society of America* A **56**, pp. 916–925, 1966.

[34] Vukosic, P., Sambles, J. R. and Lawrence, C. R., Color mixing in wing scales of a butterfly, Nature **404**, p. 457, 2000.

[35] Vukosic, P., Sambles, J. R., Lawrence, C. R. and Wakely, G., Sculpted–multilayer optical effects in two species of *Papilio* butterfly, Applied Optics **40**, pp. 1116–1125, 2001.

[36] Vukosic, P. and Sambles, J. R., Photonic structures in biology, Nature **424**, pp. 852–855, 2003.

[37] Wolff, L. B., Relative brightness of specular and diffuse reflection,' Optical Engineering **33**, pp. 285–293, 1994.